

A portable ultrahigh vacuum organic molecular beam deposition system for *in situ* x-ray diffraction measurements

K. A. Ritley, B. Krause, F. Schreiber,^{a)} and H. Dosch

Max-Planck-Institut für Metallforschung, Heisenbergstrasse 1, D-70569 Stuttgart, Germany
and Institut für Theoretische und Angewandte Physik, Universität Stuttgart, Pfaffenwaldring 57,
D-70550 Stuttgart, Germany

(Received 26 June 2000; accepted for publication 2 November 2000)

A portable UHV molecular beam deposition system has been developed for synthesis, *in situ*, and real-time x-ray diffraction measurements of organic thin films, multilayers, and superlattices. The system has been optimized for small size, while still incorporating full features necessary to achieve thin film growth under molecular beam epitaxy (MBE) conditions. It can be used independently for thin film growth, or it can be transported and mounted on standard diffractometers. Additionally, it can be docked to a stationary multipurpose MBE growth system for sample transfer, thus permitting more extensive growth and characterization. The design and performance of this system are reported, with emphasis on modifications required to deposit organic materials. To demonstrate the capabilities for real-time x-ray scattering experiments, some preliminary results of a study of epitaxial growth of 3,4,9,10-perylene-tetracarboxylic dianhydride on Ag(111) substrates are given.

© 2001 American Institute of Physics. [DOI: 10.1063/1.1336822]

I. INTRODUCTION

Several classes of organic materials form rich and complex structures with high structural perfection when grown as thin films upon suitable substrates. These include self-assembled monolayers (SAMs) such as alkanethiols on Au(111)¹⁻³ and planar aromatic compounds, such as perylene derivatives and phthalocyanines grown by organic molecular beam epitaxy.^{4,5} For example, one possible arrangement of the dye molecule 3,4,9,10-perylene-tetracarboxylic dianhydride (C₂₄O₆H₈, or PTCDA) on Ag(111) is the herringbone structure discussed in Sec. V. In these systems electrostatic intermolecular interactions and van der Waals forces are important for determining the structure.⁶ Most studies of these systems to date have been motivated by a broad range of potential applications which include optoelectronic devices, chemical sensors, coatings, etc.⁴ But these systems also hold promise for applications which exploit their elastic and epitaxial properties, such as for the elastic modification of metal or semiconductor heterostructure interlayers and for synthesis of lattice-mismatched epitaxial systems via coupling across a van der Waals bonded layer, a process which has been recently termed “xenotaxy.”⁷

The surface physics of organic thin films has been investigated with techniques such as low-energy electron diffraction (LEED) and scanning tunneling microscopy (STM). Owing to the small scattering cross sections (predominantly low electron density constituents) and frequently nontrivial crystallography of these structures, however, x-ray diffraction measurements of structural properties, growth mechanisms, and phase transition behavior have been less fre-

quently undertaken.^{2,5,8} In contrast to electron-based probes, x-ray diffraction measurements afford higher resolution and more straightforward quantitative analysis of data when multiple scattering effects can be ignored. Intensity requirements often restrict such measurements to high-intensity synchrotron facilities. Although some organic thin films are stable in air and can be measured *ex situ*, clearly experimental apparatus for combined thin film synthesis and *in situ*, real time study by x-ray diffraction is desirable.

Various diffractometer-based ultrahigh vacuum (UHV) sample chambers for *in situ* x-ray diffraction studies have been developed. These usually employ an integral beryllium window to permit the nearly unattenuated passage of the incident and scattered x-ray beams. One of the first designs was a pumpable chamber developed by Eisenberger and Marra which could be used for sample transport but lacked capabilities for sample preparation.⁹ The concept was subsequently extended by many groups to larger systems encompassing growth capabilities or more detailed surface analysis capabilities, frequently augmented with electron probes such as LEED or Auger electron spectroscopy.¹⁰⁻¹² In addition to systems which provide molecular beam epitaxy (MBE) growth capabilities, there are also novel systems which combine *in situ* x-ray measurements with other thin film growth methods: a variable pressure system (from UHV to 5 bar) used for catalysis and oxidation studies;¹³ *in situ* sputter deposition capabilities;¹⁴ and *in situ* organometallic vapor phase epitaxy (OMVPE).¹⁵

It is not obvious that all components required for the growth of organic monolayers, thin films, multilayers, and superlattices can be fitted to an UHV chamber small enough to easily fit on an x-ray diffractometer for *in situ* and real-time x-ray scattering experiments. In what follows we report the design of such a system, with features which in-

^{a)}Author to whom correspondence should be addressed; electronic mail: fschreib@dxray.mpi-stuttgart.mpg.de

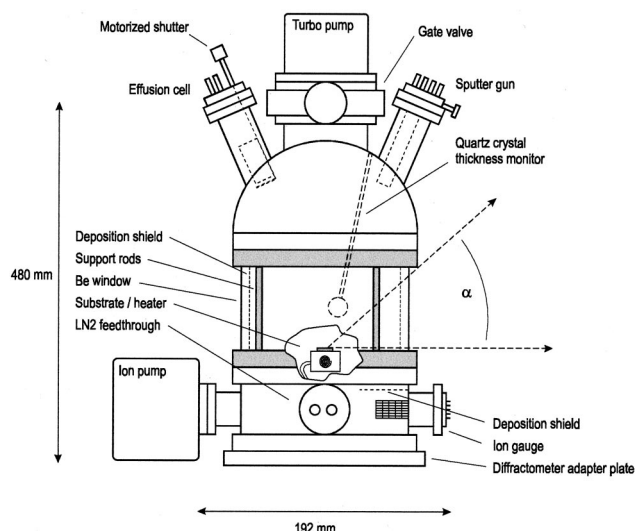


FIG. 1. A schematic diagram of the portable UHV molecular deposition system. For clarity only two of the many feedthroughs in the upper section are shown. The angle α defines the largest entrance or exit angle accessible for detecting radiation scattered from the sample.

clude (1) an integrated 360° beryllium window, making a wide variety of x-ray scattering experiments feasible; (2) complete equipment necessary for the MBE growth of organic compounds, including Knudsen-style effusion cells, a quartz crystal thickness monitor, and substrate sputtering/heating/cooling capabilities; (3) portability, by using a battery-powered ion pump so that the UHV conditions can be maintained during transport and installation of the chamber at, for example, a synchrotron beamline; and (4) relatively low cost of construction, owing to its small size. Additionally, this system can be interconnected with a stationary multichamber MBE deposition and surface-characterization system [equipped with *in situ* temperature-programmed desorption (TPD), LEED/Auger electron spectroscopy, and atomic force microscopy (AFM)/STM capabilities]. This enables more detailed synthesis and characterization of samples which can be subsequently transported under UHV conditions for measurement at laboratory x-ray sources or synchrotron/neutron facilities.

II. DESCRIPTION OF THE PORTABLE MBE SYSTEM

The system, shown schematically in Fig. 1 and in the photograph in Fig. 2, is comprised of three sections connected via standard UHV CF100 (6 in.) stainless steel flanges. The lower and upper sections each have a variety of ports for the necessary feedthroughs (power, thermocouple, cooling, evaporation sources, etc.) and accessories, described below. The upper hemispherical section required particular attention to design, in order to accommodate the four CF35 (2.75 in.) ports, the single CF63 (4.5 in.) port, and three CF16 (1.33 in.) ports on the CF100-compatible housing.¹⁶ The majority of these ports are positioned at the correct angle to afford line-of-sight with the sample surface.

The middle section contains a 1-mm-thick by 76-mm-high cylindrical Be window (Brush Wellman, Inc.) and is mounted just above the sample position. For x-ray measurements this arrangement affords a maximum $\alpha = 56^\circ$ inci-

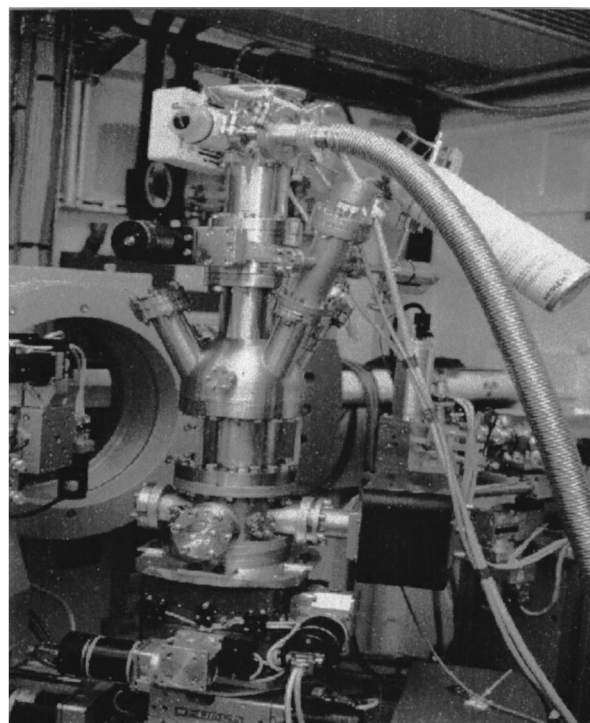


FIG. 2. Photograph of the system mounted to the Huber 6-circle surface x-ray diffractometer at Beamline ID10B at the European Synchrotron Radiation Facility (ESRF).

dence and exit angle (see Fig. 1) corresponding to a large range of out-of-plane scattering vectors $q_z = 2\pi(\sin \alpha_i + \sin \alpha_f)/\lambda$, where $\alpha_{i,f}$ are the incidence and exit angles and λ is the x-ray wavelength. Except for where three 6-mm-thick steel support posts relieve the Be window of mechanical strain, measurements throughout the full 360° azimuth are accessible. The support posts are separated asymmetrically by 112.5° and 135° rather than equally spaced at 120° to ensure that at least some in-plane x-ray reflections from samples with 60° symmetry can be measured if necessary. Additionally, it is possible to replace this middle section with one which contains an Al window, making the chamber amenable for neutron diffraction measurements.¹⁷

The system is normally pumped with a 25 l/s ion pump and a 60 l/s turbomolecular pump. Base pressures in the low 10^{-10} Torr range are readily achievable after baking the system at 150 °C. A gate valve separates the turbo pump from the system, which must be removed for sample entry or docking, discussed below. When the turbo pump is valved off, the vacuum can be maintained using the ion pump alone; a portable battery supply for the pump then renders the entire system transportable, and the ion pump current provides a measurement of the chamber pressure without the need for an ion gauge.

The samples are mounted on Riber-style 1 in. sample holders, designed to be transferred into the system vertically through the central flange on the upper chamber and then secured to the heater assembly using an interlocking bayonet mechanism. Samples can be transferred directly from air (which necessitates chamber venting and subsequent baking) or else they can be transferred under UHV conditions when the chamber is docked to the larger growth system. The sub-

strate heater (VTS/Fischer) can achieve 1000 °C via a resistively heated W filament; higher temperatures are achievable in principle with a modified design using electron beam heating.

Although the total system weight is relatively small (approximately 30–40 kg), it may require additional mechanical support, depending on the diffractometer limitations and diffraction geometry. These aspects are discussed in greater detail below. The small chamber size, in comparison with larger systems, further implies a relatively low cost of construction. The following is a brief description of other accessories contained in the chamber.

(1) Sputter gun. An Ar⁺ sputter gun mounted in the top chamber is oriented toward the sample and is used for surface preparation. The substrate can be repeatedly sputtered and annealed to obtain the desired degree of surface structural perfection, which can be verified by x-ray measurements in various diffraction geometries (rodscans, grazing incidence, etc.) before selecting the substrate temperature and proceeding with the film deposition. A small Ta “flag” located near the sample can be used to measure the sputter current when the sample is otherwise grounded by the LN₂ cooling system, described below.

(2) Deposition overspray shields. Several measures have been taken to reduce buildup of organic deposition within the system, which results from overspray from the Knudsen evaporation cells (described in Sec. III). As a long-term strategy to protect the Be window, the Be is surrounded by 10 μm ultrapure Al foil, held in place by adjustable-tension aluminum bands; this acts as an overspray shield and can be removed for cleaning or replacement. Additionally, the foil prevents overheating of the Be window when the sample is heated to high temperatures. A Ta overspray plate has been installed to shield the ionization gauge from the growth flux of the molecular sources. While usually not problematic for metal or semiconductor systems, filament-induced hydrocarbon pyrolysis may result in contamination and should be avoided. Additionally, overspray shields may be installed in the upper section of the chamber, between the effusion cells and other components (such as the sputter gun).

(3) Liquid nitrogen feedthrough. To reduce the time required for the substrate to reach room temperature following high temperature growth or annealing, or to achieve substrate temperatures below room temperature, a liquid nitrogen feedthrough which includes a small reservoir to act as a cryoshroud has been installed into the lower chamber and connected with the sample stage using copper (OFHC) braid. Substrate temperatures of about −100 °C can be obtained with the present setup. Lower temperatures can be obtained by securing the copper braid directly to a nonremovable substrate holder constructed from Cu, but in this arrangement UHV sample transfer is not possible.

(4) Mechanical counterbalance attachment. Depending on the overall resolution of the x-ray system and the nature of the intended measurements, it may be favorable to fix the sample surface either at 0° or at 90° with respect to the diffractometer sample stage. Since the sample orientation within the portable OMBE chamber is fixed, the chamber itself must be mounted on the diffractometer in one of these

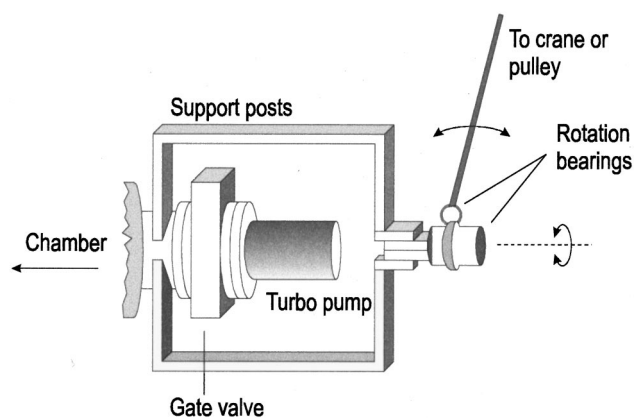


FIG. 3. A schematic diagram showing how the counterbalance support attaches to the top of the portable MBE system. A steel cable from an overhead crane or pulley is secured to the support rods via two bearings, thereby permitting limited freedom of movement as required for typical scans. An in-line spring scale visually indicates how much stress is relieved. For maximum safety it is desirable to visually inspect the support system during large diffractometer travel.

two geometries, in order to optimize the measurement conditions. For x-ray measurements with the sample and chamber in the horizontal geometry (i.e., inclined by 90° from that shown in Fig. 1), or in general to lessen the mechanical effort required by the various diffractometer circles, a counterweight/pulley system can be used. For this purpose mechanical support rods are fastened to the top of the chamber, as shown in Fig. 3. Steel cables rigged from an overhanging crane or other support are attached to rotation bearings at the end of the rods and these enable the mechanical load on the diffractometer to be relieved while permitting the free rotation of the chamber along multiple axes, as may be required by the diffraction measurements. A spring scale is attached in-line with the cables, so that the necessary counterweight can be observed and adjusted.

(5) Quartz crystal thickness monitor. A water-cooled quartz crystal thickness monitor is mounted on one of the CF35 feedthroughs. It is positioned to minimize interference with x-ray scattering experiments, sufficiently near the sample but away from the line-of-sight of the sputter gun. This sensor is capable of monitoring the areal mass density of material deposited during growth with submonolayer resolution, and is useful both for correlation with x-ray measurements and (with proper calibration) to measure deposited film thicknesses. Inasmuch as the evaporation temperatures for the organic sources are low (typically a few hundred degrees Celsius), the use of water cooling is not always necessary.

III. COMPONENTS FOR THIN FILM GROWTH

There are a large number of different preparation routes for organic thin films, such as Langmuir–Blodgett, dip/spin/spray-coating, self-assembly from solution, etc. The portable chamber facilitates two UHV-based techniques which provide optimum cleanliness and *in situ* readiness: self-assembly from vapor² and molecular beam deposition.^{4,5} In the case of SAMs formed by molecules with suitably high vapor pressure at room temperature, for example, the puri-

fied source material can be stored in a flask attached to a variable-rate leak valve. Opening the valve to achieve a precalibrated pressure results in the egress of molecules into the chamber where, under the appropriate growth conditions, they spontaneously form a highly ordered monolayer; an example of this is alkanethiol on Au(111).^{2,3}

For low-vapor-pressure materials Knudsen-type effusion cells for organic molecular beam deposition can also be used.¹⁸ There are two important constraints on their design in the present application: (1) the effusion cell should be operable at any angle and (2) the thermocouple must precisely measure the crucible temperature, established by heat conduction. In contrast to requirements for metal and semiconductor sources, the evaporation temperatures of many organic compounds are usually low (typically a few hundred °C) and therefore even slight overheating causes near total depletion of the source material. The effusion cells are designed for sublimation of organic materials and mounted into the top of the chamber, facing downwards and with line-of-sight to the substrate, as shown in Fig. 1. The organic source material is filled into high-purity alumina or quartz glass crucibles which are then densely packed with 6–12 μm diameter glass wool; the wool secures the source material to prevent spillage at any angle but affords sufficient porosity to permit the sublimed material to escape.¹⁹ The use of transparent quartz glass crucibles facilitates inspection of the amount of organic source material remaining, without the need to remove the quartz wool. Alternatively, if the organic source material is sufficiently coarse-grained, a fine metal mesh covering the crucible may be used. The thermocouple is spot-welded to a 3×3 mm Ta sheet which sits under the crucible, in order to reproducibly measure the crucible temperature. The effusion cells each have an integral shutter, which can be opened and closed remotely via an external motor mounted to the chamber. This facilitates time-resolved measurements of film growth when the chamber is located in an inaccessible x-ray hutch, such as discussed in Sec. V.

IV. DOCKING TO A STATIONARY MBE SYSTEM AND SAMPLE TRANSFER

The portable deposition system is designed for interconnectivity with a dedicated organic molecular beam epitaxy system. As shown in Fig. 4, this larger system (Omicron Instruments) contains extensive capabilities for sample growth, including effusion cells for both metal and organic evaporants, the ability to prepare self-assembled monolayers from the vapor phase, a quartz crystal thickness monitor, and a sputter gun used for preparation of single-crystal substrates. The sample manipulator can achieve temperatures between 130 and 1000 K and contains a precision linear sample shutter, so that films of multiple thickness or graded thickness (wedges) can be grown. The system also contains extensive capabilities for sample characterization, including thermal desorption spectroscopy (also known as temperature-programmed desorption, TPD), low-energy electron diffraction (LEED), *in situ* scanning tunneling microscopy (STM), contact- and non-contact mode atomic force microscopy (AFM), Auger electron spectroscopy

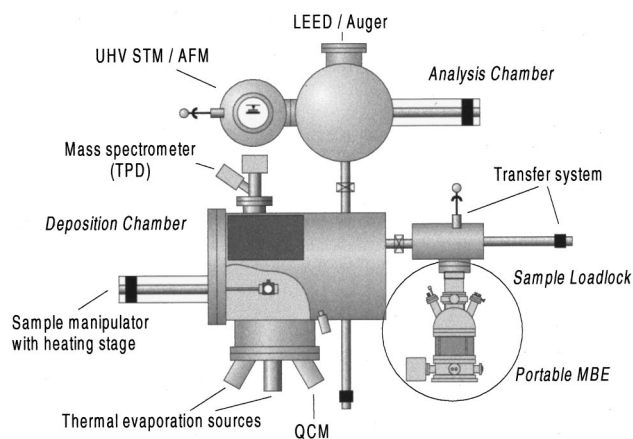


FIG. 4. Top view showing how the portable chamber (circled) docks to the loadlock section of a stationary MBE growth and analysis system. For clarity, some of the components of the growth and analysis system are omitted.

(AES), and a number of additional ports for surface-sensitive spectroscopies which are complementary to surface x-ray diffraction.

Samples can be prepared and characterized using the extensive capabilities of the larger system, then transferred under UHV conditions to the portable system for transportation to an x-ray diffractometer. This is accomplished by removing the turbo pump from the upper CF63 port and attaching the portable system to the loadlock of the stationary system using a pumpable gate valve, as shown in Fig. 4. One complication is that the larger system employs Omicron “platelet” sample holders, whereas the portable chamber requires the 1 in. Riber sample holders. Sample transfer is made possible by using a modified Riber sample holder, stored in the introduction chamber of the larger system. The smaller Omicron platelet holder can be secured to this using a “wobble-stick” vacuum manipulator located in the stationary MBE system, and subsequently transferred to the portable system.

V. INSTRUMENT PERFORMANCE

The portable OMBE system has been in use for more than one year, principally to study the epitaxial growth behavior, crystallography, phase transitions, and dewetting properties of aromatic compounds on single crystal substrates. This system makes possible *in situ* thin film growth in combination with various measurements, such as x-ray reflectivity, surface x-ray diffraction,^{20,21} high-angle “Bragg” diffraction,²² and grazing incidence x-ray diffraction.²³ A principal advantage of this system, however, is to make possible real-time measurements during growth, to obtain information about the epitaxial growth mode and evolution of morphology with film thickness. We provide one example of an *in situ*, real-time measurement made possible by this system, which involves the dye molecule 3,4,9,10-perylene-tetracarboxylic dianhydride ($\text{C}_{24}\text{O}_6\text{H}_8$, or PTCDA). This organic compound can be grown as high-quality single crystal thin films on noble metal substrates, as shown in Fig. 5(a), and it serves as a model system for understanding the growth of a large class of perylene derivatives as thin films.

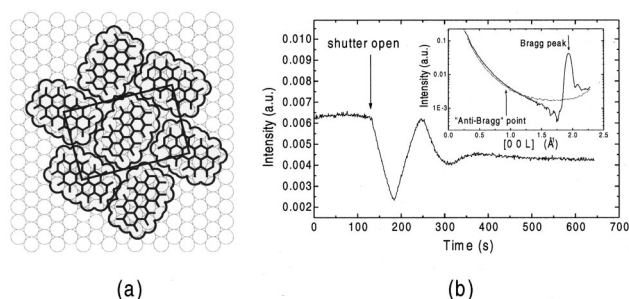


FIG. 5. (a) A schematic diagram of one possible herringbone arrangement of a monolayer of aromatic dye molecules 3,4,9,10-perylene-tetracarboxylic dianhydride ($C_{24}O_6H_8$, or PTCDA) on Ag(111) substrates, showing the orientational relationship of the unit cell with respect to the substrate. Complex epitaxial structures of organic molecules such as these are made possible by weak adhesion to the substrate and noncovalent (e.g., van der Waals, electrostatic quadrupolar interactions) between molecules. (b) The time-dependent intensity of x rays recorded during deposition of PTCDA on Ag(111), measured at the anti-Bragg location for PTCDA. The oscillations are correlated with the growth of successive monolayers, and their damping and eventual cessation indicates a transition to a growth behavior with steady-state roughness. The inset shows a comparison of intensity along the specular rod for bare (dotted line) and PTCDA-covered Ag(111) (solid line). The difference in the line shape is due to scattering interference between the thin film and substrate, which can be used to model the thin film structure. The arrow indicates the anti-Bragg PTCDA location, which is at one-half of the out-of-plane zone boundary for PTCDA.

In general, as successive adlayers accrue on the surface during deposition,^{24,25} or as buried layers are removed by interdiffusion or other mechanisms,²⁶ coverage-dependent changes in diffracted intensity can be observed. Usually, a sensitive location to measure these intensity changes is at one half of the zone boundary (the so-called “anti-Bragg point”) for the thin film.

Growth experiments to measure this effect were conducted at Beamline W1 of the Hamburg Synchrotron Radiation Laboratory (HASYLAB). These involved an Ag(111) substrate which was cleaned by repeated cycles of sputtering and annealing. PTCDA was evaporated at rates of 0.2–6 ml/min onto the clean Ag substrate, at temperatures between -70 and 200 °C. The intensity of the diffracted radiation was monitored at the out-of-plane anti-Bragg point during growth. It was found to be oscillatory during the first few monolayers and subsequently damped, as shown in Fig. 5(b). In this case, the periodicity of scattered intensity at the early stages of deposition is related to the formation of complete “wetting” PTCDA layers, and their damping derives from the onset of island development, via a Stransky–Krastanov growth mode. A detailed analysis of these data, including the results from other scattering experiments and correlation with AFM measurements, is presently underway.

ACKNOWLEDGMENTS

It is a pleasure to thank F. Adams, A. C. Dürr, C. Ern, E. Günther, B. Nickel, and W. Plenert for collaboration involving chamber construction, and B. Adams (HASYLAB), O. H. Seeck (HASYLAB), and D. Smilgies (ESRF) for collaboration involving x-ray measurements. The authors wish to thank N. Karl for providing them with purified organic compounds. They also acknowledge cooperation with S. Molitor and D. Frechen (Omicron Instruments) and A. Fischer (VTS/Crearec).

- ¹A. Ulman, *An Introduction to Ultrathin Organic Films: From Langmuir-Blodgett to Self-assembly* (Academic, Boston, 1991).
- ²F. Schreiber, A. Eberhardt, T. Y. B. Leung, P. Schwartz, S. M. Wetterer, D. J. Lavrich, L. Berman, P. Fenter, P. Eisenberger, and G. Scoles, *Phys. Rev. B* **57**, 12476 (1998).
- ³F. Schreiber, *Prog. Surf. Sci.* **65**, 151 (2000).
- ⁴S. R. Forrest, *Chem. Rev.* **97**, 1793–1896 (1997).
- ⁵P. Fenter, F. Schreiber, L. Zhou, P. Eisenberger, and S. R. Forrest, *Phys. Rev. B* **56**, 3046 (1997).
- ⁶K. Glöckler, C. Seidel, A. Soukopp, M. Sokolowski, E. Umbach, M. Böhlinger, R. Berndt and W.-D. Schneider, *Surf. Sci.* **405**, 1 (1998).
- ⁷R. Rudolf, Y. Tomm, C. Pettenkofer, A. Klein, and W. Jaegermann, *Appl. Phys. Lett.* **76**, 1101 (2000).
- ⁸In Refs. 2 and 5 a similar chamber constructed at Princeton University was used.
- ⁹P. Eisenberger and W. C. Marra, *Phys. Rev. Lett.* **46**, 1081 (1983).
- ¹⁰S. Brennan and P. Eisenberger, *Nucl. Instrum. Methods Phys. Res. A* **222**, 164 (1984).
- ¹¹J. R. Dennison, S.-K. Wang, P. Dai, T. Angot, H. Taub, and S. N. Ehrlich, *Rev. Sci. Instrum.* **63**, 3835 (1992).
- ¹²K. Whiteaker, Ph.D. thesis, University of Illinois at Urbana-Champaign, 1997.
- ¹³P. Bernard, K. Peters, J. Alvarez, and S. Ferrer, *Rev. Sci. Instrum.* **70**, 1478 (1999).
- ¹⁴A. P. Payne, B. M. Clemens, and S. Brennan, *Rev. Sci. Instrum.* **63**, 1147 (1992).
- ¹⁵S. Brennan, P. H. Fuoss, J. L. Kahn, and D. W. Kisker, *Nucl. Instrum. Methods Phys. Res. A* **291**, 86 (1990).
- ¹⁶Note that for a given height of the Be window, a smaller diameter affords a larger scattering angle; thus a CF100-based design is preferable to a CF150.
- ¹⁷J. A. Dura, C. F. Majkrzak, S. Krueger, and S. K. Satija, in *Exploration of Subsurface Phenomena by Particle Scattering*, edited by N. Q. Lam, C. A. Melendres, and S. K. Sinha (IASI, Northeast, 2000), pp. 245–260.
- ¹⁸M. A. Herman and H. Sitter, *Molecular Beam Epitaxy* (Springer, Berlin, 1996).
- ¹⁹N. Sato, K. Seki, and H. Inokuchi, *Rev. Sci. Instrum.* **58**, 1112 (1987).
- ²⁰I. K. Robinson and D. J. Tweet, *Rep. Prog. Phys.* **55**, 599 (1992).
- ²¹R. Feidenhans'l, *Surf. Sci. Rep.* **10**, 105 (1989).
- ²²V. Holý, U. Pietsch, and T. Baumbach, *High-Resolution X-ray Scattering from Thin Films and Multilayers* (Springer, Berlin, 1999).
- ²³H. Dosch, *Critical Phenomena at Surfaces and Interfaces* (Springer, Berlin, 1992).
- ²⁴E. Weschke, C. Schüssler-Langeheine, R. Meier, G. Kaindl, C. Sutter, D. Abernathy, and G. Grübel, *Phys. Rev. Lett.* **79**, 3954 (1997).
- ²⁵Y. Fujii, T. Nakamura, M. Kai, and K. Yoshida, *Surf. Sci.* **405**, L549 (1998).
- ²⁶P. A. Bennett, B. DeVries, I. K. Robinson, and P. J. Eng, *Phys. Rev. Lett.* **69**, 2539 (1992); I. K. Robinson, P. J. Eng, P. A. Bennett, and B. DeVries, *Appl. Surf. Sci.* **60**, 498 (1992).